

# Neutron scattering analysis of metamorphosed shales to constrain lithologic control on earth surface processes

Summer School on Small Angle Neutron Scattering and Neutron Reflectometry

NIST Center for Neutron Research

USANS Experiment

Alexis Navarre-Sitchler, Yun Liu



## Abstract

Ultra Small-Angle Neutron scattering (USANS) will be used to characterize porosity in metamorphosed and unmetamorphosed shales from the East River Valley in Colorado.

Various aspects of the experiment from the sample preparation and instrument setup to data treatment and interpretation will be investigated, and references are given for more in-depth study.

## 1. Introduction

Earth materials are hosts to numerous processes and products that impact modern life. Biogeochemical processing of nutrients, production of rock-derived solutes during weathering, concentrated deposition of critical minerals, and hydrocarbon maturation and production to name just a few. In these systems, the mineral substrate of rocks and soils defines open space for pathways of fluid movement and mineral precipitation and provides surfaces for microbial attachment, sorption, and mineral transformation. Heterogeneity of Earth materials, both physical and chemical, the length scales across which characteristics are exhibited (nm to meters), and the time scales across which characteristics are dynamic (seconds to millions of years) hinder our understanding of the fundamental processes that control how Earth materials behave over space and time. One particular group of Earth materials, shales, have received lots of attention due to the important role they play in the US energy economy, with significant increases in US hydrocarbon production and proven reserves coming from shale and other tight reservoirs. This recent focus on shale formations, from both a surface and subsurface perspective, highlight key knowledge gaps in our understanding of how hydrocarbon fluids are generated and move through these rocks in the subsurface (Ilgen et al., 2017); and from a different perspective: what controls geochemical behavior of these rocks at Earth's surface (Rimstadt et al., 2017).

Shales are comprised of varying proportions of phyllosilicate clay minerals (kaolinite, illite, smectite-group), framework silicate minerals (quartz and feldspar), and solid organic carbon. These fine-grained rocks dominate rock types deposited in marine settings and make up approximately 25% of all rocks exposed on continental land masses (Rimstadt et al., 2017). As a dominant rock type with relatively high concentrations of carbon, sulfur, and trace elements, shale formation and erosion consumes and releases enough of these important elements to impact the global budgets and cycles (Peucker-Ehrenbrink and Hannigan, 2000), in addition to controlling the fate and transport of many elements in the upper crust (Milliken, 2004). As we strive to develop mechanistic understanding of how the shallow subsurface of the earth operates and connects to evolution of the earth's surface through vegetation, surface, water, and erosion, the contribution of shales cannot be ignored.

In the southwest corner of Colorado, near the town of Crested Butte, long-term ecological and biological research is supported by the Rocky Mountain Biological Laboratory (RMBL). RMBL and the affiliated research sites are housed on the banks of the East River with the Cretaceous aged Mancos Shale underfoot (Figure 1). Historically, the research at this site has focused on vegetation and animal populations that live at Earth's surface and their dynamic evolution through time. This long-term research was leveraged by the Department of Energy's Lawrence Berkeley National Laboratory to develop a community research site focused on unraveling the details of how watersheds, the fundamental unit of parsing water resources on Earth's surface, operate in space and time. Research within the East River valley aims to address science questions related to watershed hydrology and biogeochemical processes that include: 1) How are fluxes and transformation of nutrients affected by sharp hydrobiogeochemical transitions? and 2) Can geochemical and remote characterization methods be used to identify critical zonation or diagnostic signatures of system behavior at the watershed scale?

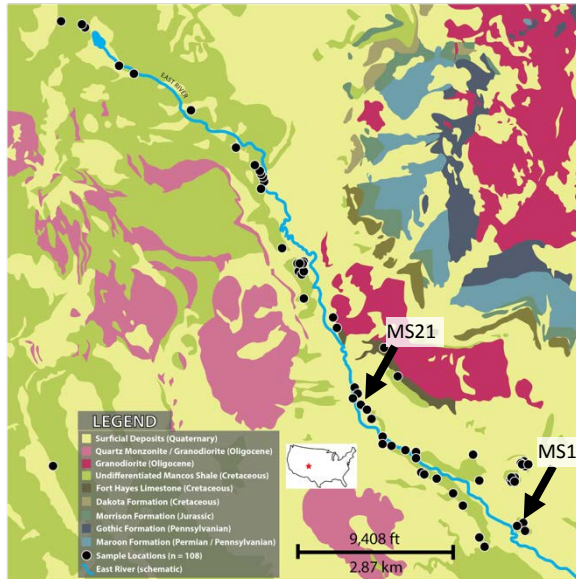


Figure 1. Map of the East River Valley with locations of samples collected. Samples for USANS Analysis during the summer school are marked with arrows.

In the East River valley, the Mancos Shale bedrock exhibits evidence of contact metamorphism along the riverbed and banks near outcropping of intrusive igneous rocks, but metamorphic grade is variable throughout the valley leading to questions of how the underlying geologic template, set by processes that occurred > 30 ma, contribute to modern watershed function. For example, in some reaches of the East River, river sinuosity is low, riverbanks are steep, and the river channel is narrow. In contrast, in some reaches river sinuosity is high, riverbanks have gradual slopes, and the river channel is wide and meandering. The distinct differences in river morphology likely control the extent and rates of hyporheic (i.e. groundwater – surface water) exchange, and thus microbial activity and associated nutrient dynamics in the river corridor (e.g., Brunke and Gonser, 1997; Packman et al., 2003; Malcolm et al., 2005; Cardenas and Wilson, 2007). The pathways

that water takes through the shale (i.e. the hydrology) and the minerals that water encounters both play important roles in (1) the release of solutes (i.e. C, S, P, N) through weathering and (2) the competence of the rock, which controls topographic expression. Metamorphism of Mancos Shale bedrock in the East River changes the mineralogy, weathering susceptibility, and pore structure, thus potentially exhibiting control on the watershed function spatially within the watershed. These variations in contact metamorphism, therefore, provide a perfect natural laboratory to investigate the range of characteristics of shale within a watershed, the evolution of those characteristics with contact metamorphism, and the role of underlying geology on modern watershed function in a shale-hosted system.

**2. How does neutron scattering help us understand the evolution of pore space in geochemically reactive systems?**

Porosity is a dynamic characteristic that provides pathways for fluid migration through rocks. The pore volume, pore size distribution, and connectivity of pores can be altered by geochemical reactions induced through weathering, diagenesis, and metamorphism. Characterizing pore space in shales is particularly difficult due to the length scales at which pores occur, often sub-mm with the majority of pores in the sub-micron size range. While imaging allows us to describe these pores and their characteristics (Figure 2), quantification of pore space in these length-scales is difficult. When combined with imaging, neutron scattering provides a powerful tool to investigate changes in pore volume, pore size distribution, and pore connectivity.

A small-angle neutron scattering experiment is carried out by measuring the scattering signal from a target sample illuminated by a collimated neutron beam with known wavelength, defined beam geometry, and calibrated neutron flux. The majority of neutrons are transmitted through the sample with

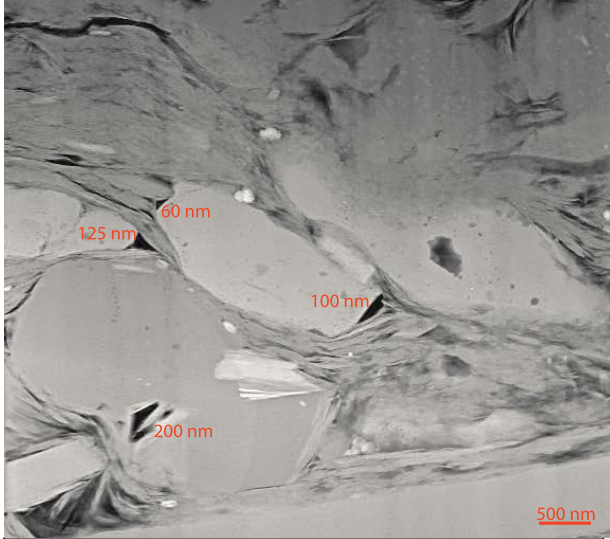


Figure 2. TEM image of pores in Gothic Shale.

no interactions, making neutron scattering suitable for the study of much larger samples compared to X-rays. A small percentage (< 10–15% is desirable) of incident neutrons are coherently scattered upon interactions with interfaces between regions with contrasts due to the difference in either chemistry or density, resulting in contrasts of scattering length density in the target sample. (Radlinski 2006). The coherent scattering length density  $\rho_j^*$  (SLD) for a solid phase  $j$  is given by Equation 1:

$$\rho_j = \frac{(\sum_{i=1}^n b_{ci})}{V_m} \quad (1)$$

Here,  $b_{ci}$  is the bound coherent scattering length of atom  $i$  of  $n$  atoms of a molecule and  $V_m$  is

the molecular volume ( $\text{g mol}^{-1}$ ). The neutron SLD does not change monotonically with atomic number, and can be very different for different isotopes of the same element. Therefore, neutrons are sensitive to certain light elements, and isotope contrast variation (especially H/D) can be utilized to highlight or suppress certain structural features in neutron scattering. The angle ( $Q$ ) at which the neutrons scatter is a function of the size ( $d$ ) of the scattering structures ( $d = 2\pi/Q$ ). Typical small-angle neutron scattering (SANS) and ultra- small-angle neutron scattering (USANS) instrument configurations used to study rocks interrogates length scales of approximately 1 nm–30  $\mu\text{m}$ . The intensity of scattered neutrons at each angle is a function of the number of scattering particles and the scattering contrast. SLD values of various minerals are generally in the range of  $4 \times 10^{10} \text{ cm}^{-2}$ , while voids (i.e., empty pores) have a SLD of zero. Thus, while neutrons also scatter from mineral grain interfaces, the intensity of scattered neutrons that arises from interfaces between minerals and pores is usually an order of magnitude higher, and rocks can often be treated as a two-phase system when analyzing neutron scattering data, i.e., minerals + pores (e.g., Radlinski 2006; Anovitz et al. 2009; Navarre-Sitchler et al. 2013). For a two-phase system, the intensity of scattered neutrons is a function of the square of SLD contrast between two materials ( $\Delta\rho^*$ ) and the volume of scattering particles, or porosity in rocks ( $\phi$ ).

$$I(Q) = (\Delta\rho)^2 \phi(1 - \phi)F(Q) \quad (2)$$

## 2.1. Experimental objective

In this experiment, samples of Mancos Shale collected from the East River valley will be analyzed using USANS, additional SANS and USANS data are available as needed. The objective is to evaluate the differences in porosity between the samples and determine if metamorphism has changed the pore network in any way.

## 2.2. Static scattering functions of a two-phase system

A two phase system can be divided in two separate regions while one region (phase 1) has a SLD,  $\rho_1$ , and another region (phase 2) has a different SLD,  $\rho_2$ , as demonstrated in Figure 3. One example is the porous material, in which the matrix is made of only one type of material. The matrix is the phase 1. And the pore space is the phase 2. (Note that here different phases are determined by the SLD only. Different materials with the same SLD are consider the same phase.)

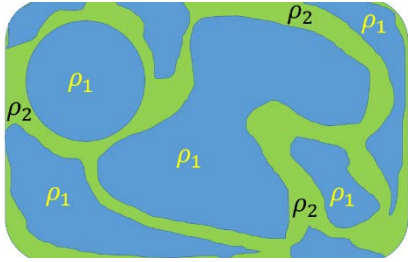


Figure 3. Schematic picture of one two-phase system

If we define the density distribution function of a system as  $\rho(\vec{r})$ , the density-density correlation function is defined as  $\gamma(\vec{r}') = \int \rho(\vec{r})\rho(\vec{r} + \vec{r}')d\vec{r}$ . Then the static scattering function measured by SANS is  $I(\vec{Q}) = \int \gamma(\vec{r}')e^{-i\vec{Q}\cdot\vec{r}'}d\vec{r}'$ . Because a disordered two phase system is typically isotropic,  $I(\vec{Q})$  and  $\gamma(\vec{r}')$  are also isotropic and can be written as  $I(Q)$  and  $\gamma(r')$ . If we assume the volume fraction for phase 1 and phase e2 are  $\phi_1$  and  $\phi_2$  respectively. It can be shown that the second moment of  $I(Q)$  is a constant that is determined by only the relative volume fraction and the contrast between two phases. This

constant is called invariant (for a two phase system), and is expressed as

$$\langle \eta^2 \rangle = \frac{1}{2\pi^2} \int Q^2 I(Q) dQ = (\rho_1 - \rho_2)^2 \phi_1 \phi_2 \quad (3)$$

Because  $\phi_1 + \phi_2 = 1$  as there are only two phases in this system, this immediately leads to

$$\langle \eta^2 \rangle = (\rho_1 - \rho_2)^2 \phi_1 (1 - \phi_1) \quad (4)$$

Hence, for a two phase system, no matter what the structures of the two phase are, the invariant always remain a constant if the contrast and volume fraction are not changed.

The normalized Porod-Debye correlation function can be thus defined as

$$\gamma_0(r) = \frac{\gamma(r) - \langle \rho \rangle^2}{\langle \eta^2 \rangle} \quad (5)$$

where  $\langle \rho \rangle$  is the average SLD of the whole system. Therefore,

$$I(Q) = \langle \eta^2 \rangle \int \gamma_0(r) e^{-i\vec{Q}\cdot\vec{r}} d\vec{r} = (\rho_1 - \rho_2)^2 \phi_1 (1 - \phi_1) F(Q) \quad (6)$$

where  $F(Q) = \int \gamma_0(r) e^{-i\vec{Q}\cdot\vec{r}} d\vec{r}$ .

Note that  $\gamma_0(r = 0) = 1$  and  $\gamma_0(r = \infty) = 0$ . One of commonly used function forms for the Porod-Debye function is  $\gamma_0(r) = e^{-r/\xi}$ , where  $\xi$  is the correlation length in a sample. (This correlation function can be found for a system close to its critical point.) The corresponding scattering function is then

$$I(Q) = (\rho_1 - \rho_2)^2 \phi_1 (1 - \phi_1) \frac{8\pi\xi^3}{(1+Q^2\xi^2)^2} \quad (7)$$

This is the well-known Debye-Anderson-Brumberger model.

If all interfaces are smooth surfaces, at high enough  $Q$ , the scattering intensity,  $I(Q)$ , follows the Porod's scattering law as  $I(Q) = 2\pi(\rho_1 - \rho_2)^2 \frac{S}{V} \frac{1}{Q^4}$ , where  $S$  is the total surface area in a sample,  $V$  is the sample volume in a neutron beam.

### 3. The USANS Instrument

Fundamentally, a SANS/USANS experiment measures the number of neutrons scattered as a function of scattering angle. Since the size probed is inversely proportional to angle, to examine larger objects, we need to measure scattering at smaller angles. In the case of a "pinhole" SANS instrument this is achieved by moving the position of a two-dimensional detector relative to the sample. The smaller angle a detector element subtends, the further the detector is from the sample.

The SANS instruments at the NCNR can measure the  $q$  value down to  $8 \times 10^{-4} \text{ \AA}^{-1}$  at their maximum sample to detector distance using lenses to focus the neutron beam. This implies a maximum size of measurable objects of approximately 500nm. One can imagine simply making longer and longer instruments to study larger and larger objects. However there are limitations to that approach. Firstly, neutrons have mass and thus are affected by gravity. They fall on a parabolic path as they travel from the source to a detector. Secondly, the collimation requirements for longer instrument reduces the neutron flux onto the sample and increase the counting times. The count rate at the detector varies with the fourth power of the resolution. There is an alternative to a pinhole instrument using crystal diffraction before and after the sample in order to determine angular changes in the scattered beam. Such an instrument design is known as a Bonse-Hart type or Double-Crystal diffractometer (see Figure 4).

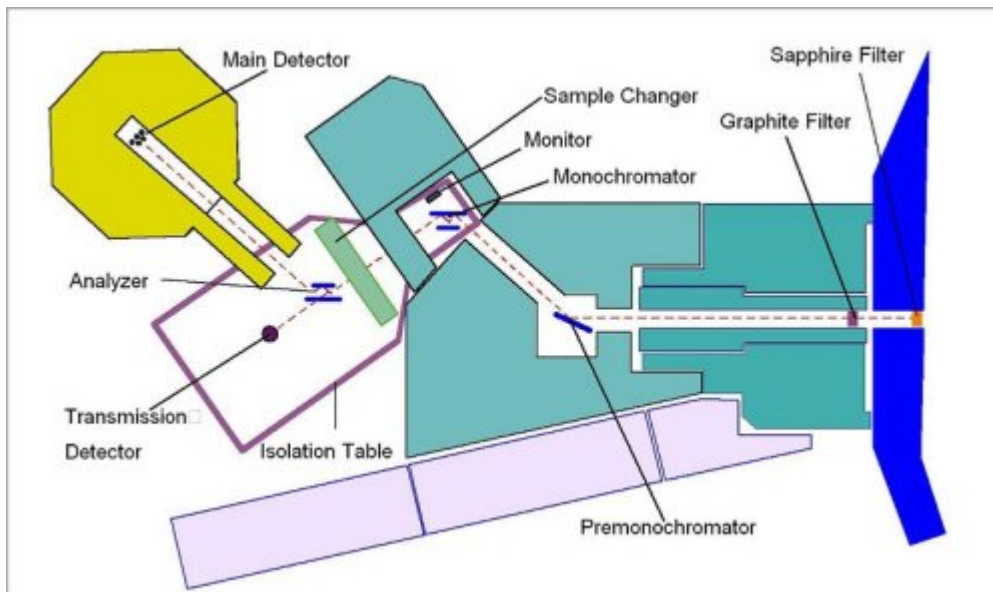


**Figure 4:** Schematic layout of the BT-5 USANS instrument. The dashed line indicates the beam path. The measured scattering angle, or momentum transfer  $q$ , is determined by rotation of the analyzer crystal.

Figure 4 shows the schematic layout of the NCNR USANS instrument which is located on beam tube 5 (BT-5). A channel cut silicon crystal (monochromator) directs the neutron beam onto the sample, where the neutrons are scattered. A second identical channel cut crystal (analyzer) is then placed in the scattered

beam path and rotated to select the scattering angle to be analyzed and diffract the neutrons scattered at that angle into the detector. An experiment consists of rotating the analyzer to a series of angles and counting the number of neutrons that reach the detector. The intensity of scattering on the detector after background correction in a USANS experiment is given by

$$I_{cor}(q) = \varepsilon I_{beam} \Delta\Omega_A d_s T \left( \frac{d\sum_s(q)}{d\Omega} \right) \quad (8)$$

where

$\varepsilon$  is the detector efficiency

$I_{beam}$  is the number of neutrons per second incident on the sample

$d_s$  is the sample thickness

$T$  is the sample transmission

$\Delta\Omega$  is the solid angle over which scattered neutrons are accepted by the analyzer

$\frac{d\sum_s(q)}{d\Omega}$  is the measured differential macroscopic scattering cross section, which is the true cross section modified by the instrumental resolution function.

The aim of a SANS/USANS experiment is to obtain the differential macroscopic scattering cross section  $\frac{d\Sigma}{d\Omega}$  from  $I_{meas}$ . How we can go through that process is described later. But first we need to decide how to prepare our sample for the measurement.

## 4. Planning the Experiment

Given the stated objectives of the experiment and knowledge of the instrument, how do we prepare the experiment to maximize our chances of scientific success? Here we discuss some of the issues that are worth considering before an experiment.

### 4.1. Scattering Contrast

In order to have enough scattering intensity, there must be scattering contrast between, in this case, materials on the two side of interface in a rock. As shown previously, the absolute intensity of the neutron scattering can be expressed as  $I(Q) = (\Delta\rho)^2 \phi_1(1 - \phi_1)F(Q)$ . Hence, the scattering is proportional to the scattering contrast,  $\Delta\rho^2$ , where

$$\Delta\rho = \rho_1 - \rho_2 \quad \leftarrow \text{Scattering Contrast} \quad (9)$$

and  $\rho_1$  and  $\rho_2$  are the scattering length densities (SLD) of the microspheres and the solvent, respectively.

$$\text{Recall that SLD is defined as } \rho = \frac{\sum_{i=1}^n b_i}{V} \quad (10)$$

where  $V$  is the volume containing  $n$  atoms, and  $b_i$  is the (bound coherent) **scattering length** of the  $i^{\text{th}}$  atom in the volume  $V$ .  $V$  is usually the molecular or molar volume for a homogenous phase in the system of interest.

The SLD of each component can be calculated from the above formula, using a table of the scattering lengths of elements [4]. (The scattering length of different elements can be found at the NCNR website: <https://www.ncnr.nist.gov/resources/n-lengths/> . [5]) Or it can be calculated using the interactive *SLD Calculator* at the NCNR's Web pages (<http://www.ncnr.nist.gov/resources/index.html>). In SANS experiments it is a common practice to deuterate one or more components to increase the contrast for the component under study. In particular, deuterating the solvent removes much of the incoherent background from the hydrogen, which is a limiting factor for many samples for measurements at high  $q$  (above  $0.2 \text{ \AA}^{-1}$ ), but this is not relevant for the USANS experiment.

Material	Chemical Formula	Mass Density (g/cc)	SLD ( $\text{cm}^{-2}$ )
Water	H <sub>2</sub> O	1.0	$-0.56 \times 10^{10}$
Heavy water	D <sub>2</sub> O	1.1	$6.33 \times 10^{10}$
Illite?			
Smectite?			
Calcite?			
Contrast matched fluid?			

**Table 1.** The scattering length densities (SLD's) for H<sub>2</sub>O and D<sub>2</sub>O with spaces to record the SLD of mineral components of shale and estimate the ratio of H<sub>2</sub>O and D<sub>2</sub>O needed for a contrast match experiment.

## 4.2. Sample Thickness

**How thick should one sample be?** Recall that the scattered intensity is proportional to the product of the sample thickness,  $d_s$  and the sample transmission,  $T$ . It can be shown that the transmission, which is the ratio of the transmitted beam intensity to the incident beam intensity, is given by

$$T = e^{-\Sigma_t d_s}, \quad (11)$$

where  $\Sigma_t = \Sigma_c + \Sigma_i + \Sigma_a$ , i.e. the sum of the coherent, incoherent and absorption macroscopic cross sections. The absorption cross section,  $\Sigma_a$ , can be accurately calculated from tabulated absorption cross sections of the elements (and isotopes) if the mass density and chemical compositions of the sample are known. The incoherent cross section,  $\Sigma_i$ , can be estimated from the cross section tables for the elements as well. The coherent cross section,  $\Sigma_c$ , can only be approximately estimated since it depends on the details of both the structure and the correlated motions of the atoms in the sample. This should be no

surprise as  $\Sigma_c$  as a function of angle is the quantity we are aiming to measure! The scattered intensity is proportional to  $d_s T$  and hence

$$I_{meas} \propto d_s e^{-\Sigma_t d_s} \quad (12)$$

which has a maximum at  $d_s = 1/\Sigma_t$  which implies an optimum transmission,  $T_{opt} = 1/e \approx 0,37$ . The sample thickness at which this occurs is known as the “1/e-length”. The NCNR web based SLD calculator provides estimates of  $\Sigma_i$  and  $\Sigma_a$  and gives an estimate of the 1/e-length as well as calculating the SLD.

### 4.3. Multiple Scattering

The analysis of small angle scattering data assumes that a neutron is scattered only once when passing through a sample so that the scattering intensity is simply related to the structure of the sample. However, if the scattering of a sample is very strong, the multiple scattering may contribute significantly to the scattering signal. The analysis of a signal with strong multiple scattering is very challenging [6] and, sometimes, is essentially impossible. Thus when  $\Sigma_c$  is significantly larger than  $\Sigma_i + \Sigma_a$  the thickness should be chosen such that the transmission due to the coherent scattering remains larger than 0.9, rather than 0.37 to avoid problems with the multiple scattering effect.

In this experiment, the samples have been prepared to a thickness of 150 microns to prevent multiple scattering based on previous work with geological samples (e.g. Anovitz et al. 2009, Jin et al. 2011, Navarre-Sitchler et al., 2013)

### 4.4. Required q range

The q range that is routinely accessible using the BT-5 USANS instrument is  $5 \times 10^{-5} \text{Å}^{-1}$  to  $5 \times 10^{-3} \text{Å}^{-1}$ . Both low q and high q limits are in practice determined by whether there is measurable scattering above background since the analyzer can be set to count at any value of q. The high q value chosen for an experiment is usually determined by the length scales of relevance to a sample and whether overlap with the SANS measurement regime is required. Figure 5 shows the accessible q ranges of the SANS and USANS instruments. In this experiment we will be measuring to approximately  $2 \times 10^{-3} \text{Å}^{-1}$ .

## 5. Collecting data

As discussed earlier, the experiment consists of scanning the analyzer through a series of angles and counting the scattered intensity on the detector. The first step before collecting the scattering data, therefore, is to decide which angles to measure at and how long to count at each.

### 5.1. Configuring the instrument

We need to measure over a range of angles spanning two orders of magnitude in  $q$  and an appropriate  $q$ -spacing at low  $q$ -values would lead to a huge excess of data points at around  $q=1 \times 10^{-3} \text{ \AA}^{-1}$ .

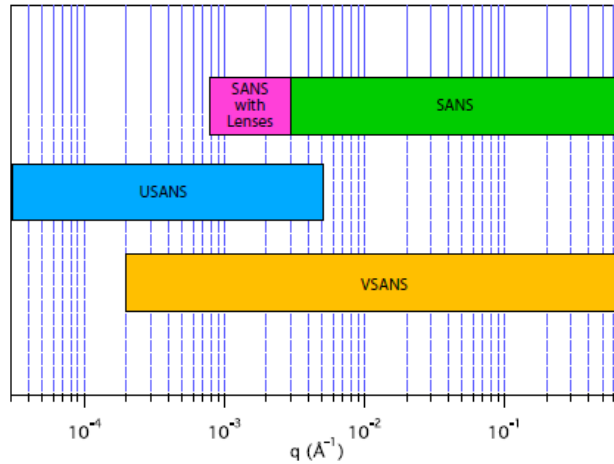


**Figure 5:** Comparison of the accessible  $q$  ranges of the BT-5 USANS instrument, NG-3 and NG-7 SANS instruments and the VSANS instrument currently under construction.

Thus we divide the data collection into six separate equally spaced scans, with each scan having roughly double the  $q$  spacing of the previous one. In the region, where the intensity varies greatly, we use closely spaced steps and increase the step size gradually as the intensity variation decreases. Furthermore, we count for short times where scattering intensity is high, and gradually increase the counting times as the intensity diminishes. The first scan spans the main beam and the peak intensity from that scan is used to determine the  $q=0$  angle, to scale the intensity into absolute units and to determine the sample transmission.

## 5.2. What measurements to make

To correct the instrument “background”, a measurement of scattering without the sample is needed. Counts recorded on the detector can come from three sources: 1) neutrons scattered by the sample itself; 2) neutrons scattering from something other than the sample, but which pass through the sample; and 3) everything else, including neutrons that reach the detector without passing through the sample (stray neutrons or so-called room background) and electronic noise in the detector itself. In order to separate these contributions we need to make three separate measurements:

1. Scattering measured with the sample in place (which contains contributions from all three sources listed above),  $I_{sam}$
2. Scattering measured with an empty sample holder in place (which contains contributions from sources 2 and 3 above),  $I_{emp}$
3. Counts measured with a complete absorber at the sample position (which contains only the contribution from source 3 above),  $I_{bgd}$

The  $I_{bgd}$  on the USANS instrument is predominantly due to fast neutrons. This background is independent of instrument configuration as the fast neutrons are not coming along the beam path. It has been measured and is  $0.018s^{-1}$ , which equals 0.62 counts per  $10^6$  monitor counts. Thus we do not usually measure a blocked beam run on USANS but use a fixed value for  $I_{bgd}$ .

### 5.3. How long to count

The uncertainty of the counting number due to the stochastic nature of the radiation (here, neutron) beam is important to understand the statistical error bar built into the scattering signal you collect. This uncertainty, or more precisely the standard deviation  $\sigma$  in the number of counts recorded in time, is given by  $\sigma = \sqrt{N(t)}$ . Here  $N(t)$  is the total number of counts at certain detector position after counting for time  $t$ . Therefore, the relative error,  $\sigma / N = 1/\sqrt{N} = 1/\sqrt{\gamma t}$ , where  $\gamma$  is the average counting rate of a sample. Thus increasing the counting time by a factor of four will reduce the relative error,  $\sigma / N$  by a factor of two. If there are 1000 total counts per data point, the standard deviation is  $\sqrt{1000}$ , which is approximately 30, giving a relative uncertainty of about 3%, which is good enough for most purposes.

A related question is how long the empty cell measurements should be counted relative to the sample measurement. The same  $\sigma = \sqrt{N(t)}$  relationship leads to the following approximate relationship for optimal counting times

$$\frac{t_{bdg}}{t_{sam}} = \sqrt{\frac{CountRate_{bgd}}{CountRate_{sam}}} \quad (14)$$

Hence if the scattering from the sample is weak, the background should be counted for as long as (but no longer than!) the sample scattering. If, however, the sample scattering count rate is, say, 4 times greater than the background rate, the background should be counted for only half as long as the sample. Since the scattering usually becomes much weaker at larger  $q$ , the time spent per data point increases with angle and the high  $q$  scans dominate the overall counting time.

### 5.4. Sample Transmission

The sample transmission is determined in two ways.

#### 5.4.1. Wide angle transmission

A separate transmission detector (see figure 4), located behind the analyzer, collects all neutrons not meeting the Bragg condition for the analyzer. When the analyzer is rotated to a sufficiently wide angle from the main beam orientation this transmission detector counts both the direct beam intensity and the coherently small angle scattered intensity. Thus the ratio of the count rate on the transmission detector

with and without the sample is the sample transmission ( $T_{wide}$ ) due to attenuation from incoherent scattering and absorption.

#### 5.4.2. Rocking curve transmission

Rotating the analyzer through the main beam allows the intensity at  $q = 0$  to be measured. The ratio of this intensity with and without the sample gives the transmission of the sample ( $T_{rock}$ ) due to attenuation from incoherent scattering, absorption and coherent small angle scattering.

#### 5.5. Multiple scattering estimate

The ratio of these separate transmission measurements can be used to estimate the amount of multiple scattering by

$$T_{SAS} = \frac{T_{Rock}}{T_{Wide}} = e^{-\tau} \quad (15)$$

If  $T_{SAS} > 0.9$ , the multiple scattering effect can be safely ignored. However, if  $T_{SAS} < 0.9$ , the multiple scattering becomes a concern.

#### 5.6. Simulation of Scattering

Given enough information about the chemical composition of the sample and expected scattering properties, we can simulate the scattering to help us optimize the experimental setup. The reduction and analysis package provided by NCR [6, 7] contains tools to help you do this.

The simulation takes input about your sample and simulates the data you would expect to collect on the instrument. This can guide you in deciding many of the factors discussed above such as appropriate sample thickness, counting time, and amount of multiple scattering. Additionally, it can help decide on the density of data points to be collected for USANS or the instrument configurations for SANS.

### 6. Data reduction

Data reduction consists of correcting the measured scattering from the sample for the sources of background discussed in section 5.2 and rescaling the observed, corrected data to an absolute scale of scattering cross section per unit volume. This is done via equation (8) presented previously and reproduced here for reference:

$$I_{cor}(q)_s = \varepsilon I_{beam} \Delta\Omega_A d_s T\left(\frac{d\sum_s(q)}{d\Omega}\right) \quad (16)$$

The beam intensity  $\varepsilon I_{beam}$  is measured by rotating the analyzer through the direct beam at  $q = 0$  with the empty cell in the beam path. The transmission  $T$  is measured by taking the ratio of the count rate observed

on the transmission detector with and without the sample in the beam path. The solid angle of scattering accepted by the analyzer  $\Delta\Omega_A$  is given by

$$\Delta\Omega_A = \left(\frac{\lambda}{2\pi}\right)^2 (2\Delta q_v)\Delta q_h, \quad (17)$$

where  $2\Delta q_v$  is the total vertical divergence of the beam convoluted with the angular divergence accepted by the detector and  $\Delta q_h$  is the horizontal divergence accepted for the diffraction by monochromator and analyzer crystals. The instrument accepts scattered neutrons with  $\pm\Delta q_v=0.117\text{\AA}^{-1}$ . The horizontal resolution  $\Delta q_h$  is measured from the full width at half maximum (fwhm) of the main beam profile obtained by rotating the analyzer through the direct beam. The fwhm when the crystal is properly aligned is  $2.00\text{ arcsec}$ , equating to  $\Delta q_h = 2.55 \times 10^{-5} \text{\AA}^{-1}$  (the BT-5 instrument uses a mean wavelength  $\lambda=2.38\text{\AA}$ ), thus the solid angle over which neutrons are accepted by the analyzer is  $\Delta\Omega_A = 8.6 \times 10^{-7} \text{ ster}$ .

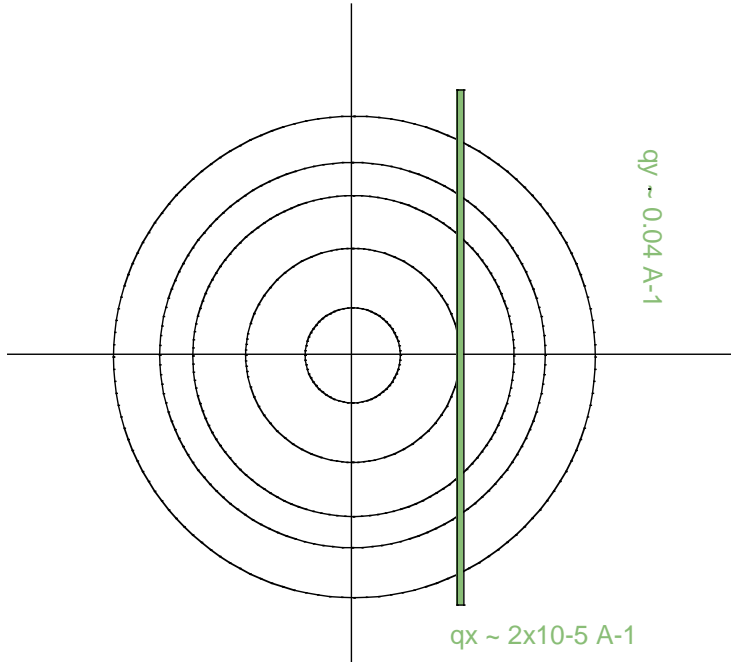


**Figure 6:** View of scattering with axes  $q_x$  and  $q_y$  collected by the analyzer on the BT-5 USANS instrument. The circles represent iso-intensity contours from isotropic small angle scattering. The narrow slit represents the scattering region collected by the analyzer.

As you may have noted above, the analyzer has very good resolution in the horizontal direction and very poor resolution in the vertical direction as depicted graphically in figure 6. This is referred to as “slit geometry” as opposed to the “pinhole geometry” of a standard SANS instrument – you may be familiar with this from using a Kratky camera for lab-based small angle x-ray scattering. The large difference between the horizontal and vertical resolutions means that the smearing can be treated as that from an

“infinite” slit. The measured cross section,  $d\Sigma_s / d\Omega(q)$  obtained from data reduction as described above is related to the true differential macroscopic cross section,  $d\Sigma / d\Omega(q)$  by the relation [8]:

$$\frac{d\Sigma_s}{d\Omega(q)} = \frac{1}{\Delta q_v} \int_0^{\Delta q_v} \frac{d\Sigma}{d\Omega} (\sqrt{q^2 + u^2}) du \quad (18)$$

Figure 7 compares the scattering from a 1 % volume fraction dispersion of 2  $\mu\text{m}$  silica particles with 5% polydispersity in  $\text{D}_2\text{O}$  using pinhole and slit geometries. Note the damping of the oscillations, the change in slope and reduction in intensity. Desmearing the data directly can be done by an iterative convergence method[Lake, J. 1967] but the desmeared result is very unstable, being sensitive to noise in the data. The preferred method is to make use of equation (18) to smear a model function and fit the smeared data directly. The latter is the method we will employ in the analysis of our data.

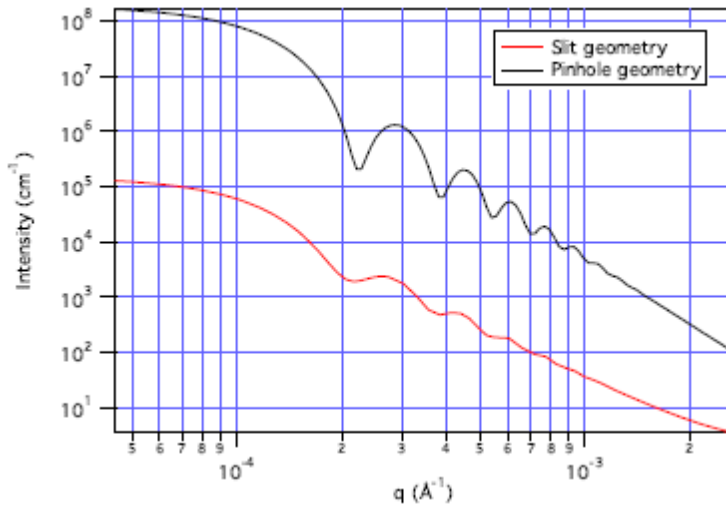


**Figure 7:** Comparison of the modeled scattering from a 1 % volume fraction dispersion of 2  $\mu\text{m}$  silica particles with 5% polydispersity in  $\text{D}_2\text{O}$  using pinhole and slit geometries.

## 7. Data Analysis

At the summer school we will use the IGOR USANS/SANS package to reduce data collected and generate scattering intensity ( $I(Q)$ ,  $\text{cm}^{-2}$ ) as a function of  $Q$  (scattering vector,  $\text{\AA}^{-1}$ ) for analysis. You will be provided the corresponding SANS data in order to analyze a full scattering curve.

Since hydrogen in rock samples produces incoherent scattering at all  $Q$  values, this  $I(Q)$  contribution from incoherent scattering must be estimated by fitting a power law (equation 19) to the long tail of constant

intensity at high  $Q$  ( $c$  in equation 13) and subtracted from the intensity at all  $Q$  values prior to further analysis.

$$I(Q) = aQ^{-m} + c \quad (19)$$

After subtracting the incoherent background, the data can then be plotted on Porod plots ( $\log I(Q) \cdot Q^4$  vs.  $\log Q$ ) to enhance differences in the power law dependence of  $I(Q)$  on  $Q$  (the apparent slope of the data on a scattering diagram). Scattering data from linear regions over  $> 1$  order of magnitude in  $Q$  identified on the Porod diagrams indicate fractal distributions within the sample and the data can be fit with a power law (Equation 20) to evaluate fractal dimensions.

$$I(Q) = aQ^{-m} \quad (20)$$

The resulting power (or apparent slope,  $m$ ) can then be used to calculate the fractal dimension, where  $2 < m < 3$  corresponds to a mass fractal dimension,  $D_m$ , and  $3 < m < 4$  corresponds to a surface fractal dimension,  $D_s$ , and:

$$\begin{aligned} D_m &= m \\ D_s &= 6 - m. \end{aligned} \quad (21a,b)$$

The porosity of the sample can be estimated by calculating  $Q_{inv}$  through equation 22. In order to calculate the total porosity assumptions must be made about the Intensity as a function of  $Q$  outside of the USANS range. For this exercise when you calculate the invariant state your assumptions.

$$Q_{inv} = \int_0^{\infty} Q^2 I(Q) dQ = 2\pi^2 \langle \eta^2 \rangle = 2\pi^2 (\Delta\rho)^2 \phi(1 - \phi) \quad (22)$$

Sample surface area can be estimated from the Porod diagram (Radlinski et al., 1996). Equation 23 is used to calculate the smooth surface area ( $S_0$ ),

$$S_0 = \frac{a}{2\pi(\Delta\rho)^2}. \quad (23)$$

Where  $a$  is the y-intercept of a flattened region at low  $Q$  on the Porod plot and  $\Delta\rho$  is the difference in scattering length density between pores and minerals. The surface fractal dimension ( $D_s$ ), determined from the scattering plot, is then used to estimate the rough surface area ( $S_r$ ) with equation AC,

$$S_r = S_0 \left( \frac{r}{\xi} \right)^{2-D_s} . \quad (24)$$

Where  $r$  is the scale of the roughness and  $\xi$  is the correlation length, which you can estimate at  $\sim 5$  nm and  $\sim 7.5$  nm, respectively.

## 8. Summary

Through this experiment you shall learn the following concepts and understand how to apply them to gain useful information from your measurements:

### Objectives of the Experiment:

- Get familiar with the USANS technique, how to optimize a sample for USANS and extract useful information from USANS scattering
- Evaluate the pore structure and network of a rock sample using neutron scattering
- Calculate the porosity of a rock sample from scattering data.

### References:

- Anovitz, L.M., Lynn, G.W., Cole, D.R., Rother, G., Allard, L.F., Hamilton, W.A., Porcar, L., Kim, M.H., 2009. A new approach to quantification of metamorphism using ultra-small and small angle neutron scattering. *Geochimica Et Cosmochimica Acta* 73, 7303-7324.
- Brunke, M. & Gonser, T. (1997). The ecological significance of exchange processes between rivers and groundwater. *Freshw. Biol.* **37**, 1–33.
- Cardenas, M. B. & Wilson, J. L. (2007). Exchange across a sediment-water interface with ambient groundwater discharge. *J. Hydrol.* **346**, 69–80.
- Ilgen, A.G., Heath, J.E., Akkutlu, I.Y., Bryndzia, L.T., Cole, D.R., Kharaka, Y.K., Kneafsey, T.J., Milliken, K.L., Pyrak-Nolte, L.J., Suarez-Rivera, R., 2017. Shales at all scales: Exploring coupled processes in mudrocks. *Earth-Science Reviews* 166, 132-152.

- Jin, L., Rother, G., Cole, D.R., Mildner, D., F.R., Duffy, C.J., Brantley, S.L., 2011. Characterization of deep weathering and nanoporosity development in shale - a neutron study. *American Mineralogist* 96, 498-512.
- Malcolm I.A., Soulsby, C., Youngson A.F., & Hannah, D.M. (2005). Catchment-scale controls on groundwater-surface water interaction in the hyporheic zone: Implication for salmon embryo survival, *River Res. and Appl.*, **21**, 977–989.
- Milliken, K. L., 2004, Chapter 5. Elemental transfer in sandstone-shale sequences, *in* Mackenzie, T., ed., *Sediments, diagenesis, and sedimentary rocks*, v. 7, *Treatise on geochemistry*: Elsevier, p. 159–190.
- Navarre-Sitchler, A.K., Cole, D., Rother, G., Jin, L., Buss, H.L., Brantley, S.L., 2013. Porosity and surface area evolution during weathering of two igneous rocks. *Geochimica Et Cosmochimica Acta*.
- Packman A. I. & Salehin M., (2003). Relative roles of stream flow and sedimentary conditions in controlling hyporheic exchange. *Hydrobiologia*, **494**, 291–297.
- Peucker-Ehrenbrink B and RE Hannigan (2000) Effects of black shale weathering on the mobility of rhenium and platinum group elements. *Geology*, **28**, 475-478.
- Radlinski, A.P., Boreham, C.J., Wignall, G.D., Jin, J.-S., 1996. Microstructural evolution of source rocks during hydrocarbon generation: A small-angle-scattering study. *Physical Review B* 53, 14 153.
- Radlinski, A.P., 2006. Small-angle neutron scattering and the microstructure of rocks, in: Wenk, H. (Ed.), *Neutron Scattering in Earth Sciences*. Mineralogical Society of America, pp. 363-397.
- Rimstidt, J.D., Chermak, J.A., Schreiber, M.E., 2017. Processes that control mineral and element abundances in shales. *Earth-Science Reviews* 171, 383-399.
- Lake, J. 1967, An iterative method of slid-correcting small angle X-ray data, *Acta. Cryst.*, **23**, 191-194